

Requirements for Cosmological 21cm Masers

Mark Dijkstra^{1*} and Abraham Loeb^{2†}

¹*School of Physics, University of Melbourne, Parkville, Victoria, 3010, Australia*

²*Astronomy Department, Harvard University, 60 Garden Street, Cambridge, MA 02138, USA*

25 May 2019

ABSTRACT

We explore the prospects for a population inversion in the hyperfine levels of atomic hydrogen at high redshifts when the Universe was still predominantly neutral. The existence of 21-cm masers during the epoch of reionisation (EoR) could greatly boost the expected EoR signals. We show that the color temperature of Ly α photons emitted by a bright source embedded in a neutral collapsing gas cloud may be sufficiently negative to establish population inversion in the hyperfine transition via the Wouthuysen-Field effect. In practice, however, a small flux of Ly α photons produced via x-ray heating or through cascades of atoms which are photo-excited by higher Lyman-series photons, can counteract this effect. In order for maser conditions to prevail, the spectrum of the source must be strongly suppressed blueward of the Ly β transition. We specify conditions in a clumpy two-phase interstellar medium (ISM), which could give rise to the required spectrum. We find that the most likely sites for 21-cm masers are cold infall regions around galaxies undergoing massive star formation ($\dot{M} \gtrsim 10^3 M_\odot \text{ yr}^{-1}$), obscured from view by a large column of gas with $N_{\text{H}} \gtrsim 10^{22.5} \text{ cm}^{-2}$ (reminiscent of known starburst galaxies at lower redshifts). Crucial for the existence of masers is for the dust in the ISM to be locked-up in cold dense clumps embedded in a hot tenuous medium, through which a large fraction of the emitted Ly α photons can escape the galaxies.

Key words: cosmology: theory—radiative transfer—galaxies: high-redshift

1 INTRODUCTION

Detecting the redshifted HI 21-cm line from the epoch of reionisation is among the greatest observational challenges in present-day cosmology. Experiments such as the Low Frequency Array (LOFAR)¹, the Primeval Structure Telescope (PAST, Peterson et al. 2006) and the Mileura Widefield Array (MWA)², are currently being developed with the goal to detect this *Epoch of Reionisation* (EoR) signal within the next few years.

The strength and sign of the EoR signal depend on the spin temperature of the hydrogen gas, T_s , which is defined through the ratio of atoms in the ground and excited states of the hyperfine transition in the electronic ground state of hydrogen, $n_2/n_1 \equiv g_2/g_1 \exp[-T_*/T_s]$, where the ground and excited states are denoted by the labels '1' and '2', respectively and $T_* = 0.068 \text{ K}$. If we denote the temperature of the Cosmic Microwave Background (CMB) by T_{CMB} , then neutral hydrogen gas can be seen in emission if $T_s > T_{\text{CMB}}$.

When $T_s < T_{\text{CMB}}$, the neutral hydrogen gas can be seen in absorption against the the CMB.

The distribution of atoms in the hyperfine levels is affected by collisions among the atoms as well as absorption and re-emission of the Cosmic Microwave Background (CMB) photons. Because of these interactions, the spin temperature is a weighted mean of T_{CMB} and T_{gas} (the gas temperature), where the weight of each is determined by the rates at which atoms collide and CMB photons are absorbed (Scott & Rees 1990; Loeb & Zaldarriaga 2004). At $z \gtrsim 200$ Thomson scattering by residual free electrons off the CMB keeps the gas, CMB and the spin temperatures nearly equal (Peebles 1993). Below this redshift, the gas adiabatically cools more rapidly than the CMB. At high enough redshifts, collisions are abundant and the spin temperature is locked to the gas temperature until at $z \lesssim 30$ the spin temperature rises back to the CMB temperature (see Fig.1 of Loeb & Zaldarriaga 2004).

The gas temperature and density increases in objects that collapse adiabatically, and the first gravitationally-bound *mini-halos* may be detectable in 21-cm emission (e.g. Iliev et al. 2002). The physics becomes more complex once the first sources form. The ionizing photons emitted

* E-mail:dijkstra@physics.unimelb.edu.au

† E-mail:aloeb@cfa.harvard.edu

¹ www.lofar.org

² http://www.haystack.mit.edu/ast/arrays/mwa/site/index.html

by these sources photo-ionise the gas in their immediate surroundings. Various processes, such as x-ray heating (Venkatesan et al. 2001; Pritchard & Furlanetto 2006) and shock heating (Furlanetto & Loeb 2004) may heat neutral gas surrounding these HII bubbles to temperatures well above the CMB temperature (Furlanetto 2006). At this epoch, an additional process that may mix the populations in the hyperfine levels is through absorption and re-emission of Ly α photons, that were either emitted by nearby sources, produced as local recombination emission, or in cascades following photo-excitation by photons with energies $E \in [10.2-13.6]$ eV (Pritchard & Furlanetto 2005). When the Ly α scattering rate dominates the collisional and CMB scattering rate, the hydrogen spin temperature, T_s , approaches the Ly α color temperature, T_α (Wouthuysen 1952). Field (1959) showed that resonant scattering of Ly α photons through an optically thick medium, redistributes the photons in frequency space according to a thermal distribution in a narrow region around the line center, making $T_\alpha = T_{\text{gas}}$. This is known as the ‘Wouthuysen-Field’ (hereafter WF) effect. Because of this effect, it is commonly assumed that the presence of Ly α photons strengthens the coupling of the spin to the gas temperature (also see Hirata 2006, for a more detailed calculation) and that the neutral hydrogen gas is detectable in emission around the HII regions.

In this paper, we examine whether physical conditions exist under which the WF-effect produces population inversion (i.e. $T_s < 0$) in the hyperfine levels. The possibility of population inversion and the accompanying stimulated 21-cm emission has not been addressed in previous work related to EoR signals. Varshalovich (1967) has pointed out that the WF effect could produce population inversion in the presence of strongly anisotropic Ly α emission, or when very steep cut-offs exist in the UV spectrum blueward of the Ly α line (also see Kaplan et al. 1979, for some more exotic mechanism). The first condition is difficult to meet due to the large optical depth to Ly α photons of a neutral IGM. Exploring in more detail whether $T_s < 0$ barely needs justification: if high redshift 21-cm masers exist, they could boost the 21-cm EoR signal by orders of magnitude.

Since the WF-effect involves scattering of Ly α photons through an optically thick medium, a proper treatment of the Ly α radiative transfer is necessary. Previous work on the WF-effect generally assumed the spatial and time derivatives in the Ly α radiative transfer equation to be zero. Without these assumptions the transfer problem becomes analytically intractable. In this paper, we demonstrate that astrophysical situations may exist, during which these assumptions are no longer valid to the extent that the Ly α color temperature may, in fact, be temporarily negative. We investigate whether this may lead to detectable 21-cm masers.

The outline of this paper is as follows. In § 2 we calculate the gain factor associated with a negative hydrogen spin temperature. In § 3 we show how the standard definition of the Ly α color temperature can be extended to an arbitrary Ly α frequency distribution and how it affects the hydrogen spin temperature. In § 4 we give a simple example of a situation in which the Ly α color temperature is negative. This

is followed in § 5 and § 6 by a discussion on what astrophysical conditions are required to produce 21-cm masers and whether these are met by conventional sources. Finally, in § 7 we present our conclusions. The parameters for the background cosmology used throughout this paper are $\Omega_m = 0.3$, $\Omega_\Lambda = 0.7$, $\Omega_b = 0.044$, and $h = 0.7$ (Spergel et al. 2003).

2 THE GAIN FACTOR ASSOCIATED WITH A NEGATIVE SPIN TEMPERATURE

When $T_s < 0$, stimulated emission of 21-cm emission occurs. Here, we estimate the implications for the expected gain in the total 21-cm emissivity. The change of the intensity in the line center of the 21-cm line, I , with distance, s , is given by (Rybicki & Lightman 1979),

$$\frac{dI}{ds} = -\alpha I + j, \quad (1)$$

where α is the opacity of the gas to radiation at a wavelength of $\lambda_S = 21\text{cm}$ and j is its corresponding volume emissivity. The standard solution to this equation is

$$I(s) = I(0) e^{-\alpha s} + \frac{j}{\alpha} (1 - e^{-\alpha s}). \quad (2)$$

Here, $I(0)$ is the intensity of the 21-cm photons before they enter the gas, $I(0) = 2kT_{\text{CMB}}/\lambda_S^2$. The 21-cm volume emissivity, j , and opacity, α , are given by

$$\begin{aligned} j &= \frac{h\nu_S}{4\pi\Delta\nu_S} n_2 A_{21} \\ \alpha &= \frac{h\nu_S}{4\pi\Delta\nu_S} B_{21} (3n_1 - n_2) \approx \frac{3}{32\pi^{3/2}} \frac{T_*}{T_s} n_H A_{21} \frac{\lambda_S^3}{v_{\text{th}}}, \end{aligned} \quad (3)$$

where $\nu_s = 1.4$ Ghz, is the frequency of the hyperfine transition; $\Delta\nu_S = \nu_s v_{\text{th}}/c$, in which v_{th} is the thermal velocity dispersion of the atoms; A_{21} and B_{21} are the Einstein coefficients associated with the hyperfine transition. We used $B_{21} = A_{21} c^2 / 2h\nu_0^3$, $n_H \sim n_1/4$ and the definition of the spin temperature (§ 1) to rewrite the expression for α . Eq. (2) can be rewritten as

$$I(s) = I(0) e^{s/R_M} - \frac{2kT_s}{\lambda_S^2} (e^{s/R_M} - 1), \quad (4)$$

where $R_M \equiv -1/\alpha$, and we used that $j/\alpha = 2kT_s/\lambda_S^2$. Since for a negative spin temperature $\alpha < 0$, $I(s)$ increases exponentially with s . R_M is the length scale over which $I(s)$ increases by one factor of e and can be written as

$$\begin{aligned} R_M \equiv -\frac{1}{\alpha} &\approx 0.7 \left(\frac{1+z}{11} \right)^{-3} \left(\frac{1+\delta}{20} \right)^{-1} \\ &\times \left(\frac{T_s}{-10 \text{ K}} \right) \left(\frac{T_{\text{gas}}}{10 \text{ K}} \right)^{1/2} \text{ kpc}. \end{aligned} \quad (5)$$

Equation (5) shows that a reasonably small region in which $T_s < 0$, also known as the ‘masing region’, could produce a significant boost in $I(0)$. According to Eq. (5), the total maser amplification increases toward lower T_{gas} and $|T_s|$ values and higher densities.

3 THE LY α COLOR AND HYDROGEN SPIN TEMPERATURE

3.1 The Ly α Color Temperature

Madau et al. (1997) defined the color temperature to be:

$$\frac{kT_\alpha}{h} = - \left[\frac{\partial \log \mathcal{N}_\nu}{\partial \nu} \right]^{-1} \approx - \left[\frac{1}{J_\alpha(\nu)} \frac{\partial J_\alpha(\nu)}{\partial \nu} \right]^{-1}, \quad (6)$$

where $\mathcal{N}_\nu = c^2 J_\alpha(\nu) / 2h\nu^3$ is the photon occupation number.³ As is shown in Appendix A2, the more general expression for the Ly α color temperature that is relevant for the WF-effect, is:

$$\frac{kT_\alpha}{h} = - \frac{\int J_\alpha(\nu) \phi(\nu) d\nu}{\int \frac{\partial J_\alpha(\nu)}{\partial \nu} \phi(\nu) d\nu} = \frac{\int J_\alpha(\nu) \phi(\nu) d\nu}{\int \frac{\partial \phi(\nu)}{\partial \nu} J_\alpha(\nu) d\nu} \quad (7)$$

(which has also been derived by Meiksin, 2006, Eq. 16).⁴ Here, $\phi(\nu)$ is the normalised line profile, $\int \phi(\nu) d\nu = 1$ (e.g. Rybicki & Lightman 1979). In this paper, we will often express the frequency, ν , in terms of a dimensionless frequency variable, $x \equiv (\nu - \nu_0) / \Delta\nu_D$, where $\Delta\nu_D = \nu_0 v_{th} / c$. A negative/positive value of x corresponds to a Ly α photon that is redshifted/blueshifted with respect to the line center, respectively. When expressed as a function of x , $\phi(x) \sim e^{-x^2}$ in the ‘core’ and $\phi(x) \sim a / [\sqrt{\pi} x^2]$ in the ‘wing’ of the line. Here, a is the Voigt parameter, which is given by $a = A_\alpha / 4\pi \Delta\nu_D = 4.7 \times 10^{-4}$ (13 km s $^{-1}$ / v_{th}), where A_α is the Ly α Einstein-A coefficient. The transition frequency, x_t , between core and wing is defined by $e^{-x_t^2} = a / [\sqrt{\pi} x_t^2]$. Since $\phi(\nu)$ is strongly peaked around the line center, photons in this frequency range usually dominate the contribution to the integral.

Since $\partial\phi/\partial\nu < 0$ for $\nu > \nu_0$, simplistically $T_\alpha < 0$ when there are more photons with $\nu > \nu_0$ than with $\nu < \nu_0$. However, as mentioned in § 1, repeated scattering of photons in the line core rearranges the photons in frequency such that $T_\alpha \rightarrow T_{\text{gas}}$ (Field 1959). The situation is different for photons in the far wing of the line profile, $|x| \gg 1$. Here, the probability that a photon is scattered from frequency x back into the line core in a single scattering event is extremely small (e.g. Hummer 1962). Scattering moves the photons back to the line center by an average amount of only $-1/x$ (Osterbrock 1962). Therefore, once a photon finds itself far in the line wing, it can stay there for $\sim x^2$ scattering events (Adams 1972). For a population of Ly α photons all of which are in the blue wing of the line: (i) $T_\alpha < 0$, and (ii) scattering does not immediately redistribute the photons in frequency space such that $T_\alpha \rightarrow T_{\text{gas}}$. Therefore, a blueshifted Ly α line

³ Note that we have omitted the $3/\nu$ -term on the right-hand-side. This is only correct when $\frac{3k|T_\alpha|}{h\nu_\alpha} \sim (|T_\alpha|/3 \times 10^4 \text{ K}) \ll 1$.

⁴ The derivation of Eq. (7) does not account for the quantum interference term, which was derived for Raman scattering by Hirata (2006, his Eq. B.18). The presence of such a term would strongly reduce the probability that a spin-flip occurs through scattering by Ly α wing photons. However, this quantum interference effect might be different for the situation in which a real Ly α photon is absorbed into a particular 2p-level of hydrogen, followed by re-emission (Zygelman, private communication). This illustrates the importance of accurate atomic physics calculations (Zygelman 2006) for the problem under discussion. Here, we focus on the traditional approach to calculating the WF effect.

has the potential to sustain a negative color temperature while it interacts with the gas. This may lead to a negative spin temperature, as we discuss next.

3.2 The Hydrogen Spin Temperature

The generalised expression for the equilibrium Hydrogen spin temperature is (see Appendix A2)

$$\frac{T_s}{T_*} = \frac{1 + \frac{C_{21}}{A_{21}} + \frac{B_{21}}{A_{21}} I_{\text{CMB}} + \frac{b_1}{A_{21}}}{1 + \frac{b_1 T_*}{A_{21} T_\alpha} + \frac{C_{21} T_*}{A_{21} T_{\text{gas}}}}. \quad (8)$$

Here, A_{21} and B_{21} are the Einstein rate coefficients and C_{21} is the collisional de-excitation rate. This expression differs only slightly from the standard expression (e.g. Madau et al. 1997), in which $b_1 = 4P_\alpha/27$, where P_α is the Ly α scattering rate. Here, b_1 has an additional weak, and practically negligible, dependence on the exact Ly α spectral shape (see Eq. A12).⁵ The denominator of Eq. 8 shows that $T_s < 0$ requires $P_\alpha > 27/4(T_\alpha/T_*)A_{21} \sim 3 \times 10^{-11} \text{ s}^{-1}(T_\alpha/[-100 \text{ K}])$, provided that the Ly α scattering rate dominates the collision rate and the CMB scattering rate. Since our Ly α photons are in the line wings, their scattering cross section is significantly reduced. To get the necessary Ly α scattering rate requires a large Ly α flux. This is most easily demonstrated by writing the Ly α scattering rate as

$$P_\alpha = \frac{\sigma_0}{h\nu_0} \frac{L_{\text{Ly}\alpha}}{4\pi r^2} \int \mathcal{J}(x) \phi(x) dx, \quad (9)$$

where $\mathcal{J}(x)$ is the normalised spectrum, ($\int \mathcal{J}(x) dx = 1$). For a source emitting a top hat Ly α spectrum with $J(x) = 0$ for $x < x_{\text{min}}$ and $x > x_{\text{max}}$, the scattering rate at a distance r is

$$P_\alpha = \frac{\sigma_0}{h\nu_0} \frac{L_{\text{Ly}\alpha}}{4\pi r^2} \frac{\int_{x_{\text{min}}}^{x_{\text{max}}} \phi(x) dx}{x_{\text{max}} - x_{\text{min}}} \approx 2.6 \times 10^{-11} \text{ s}^{-1} \times \left(\frac{300 \text{ K}}{T_{\text{gas}}} \right) \left(\frac{10 \text{ kpc}}{r} \right)^2 \left(\frac{L_\alpha}{10^{44} \text{ ergs}^{-1}} \right) \left(\frac{10^5}{x_{\text{min}} x_{\text{max}}} \right), \quad (10)$$

where L_α is the total Ly α luminosity. For $x_{\text{min}} x_{\text{max}} = 10^5$, which is a reasonable choice (§ 4 and § 6), the total Ly α luminosity must exceed $10^{44} \text{ erg s}^{-1}$, which is an order of magnitude brighter than the Ly α luminosities that are typically observed in high-redshift ($z = 6.5$) galaxies (Rhoads et al. 2004; Kashikawa et al. 2006) but fainter than that of bright quasars (Fan et al. 2006).

4 AN ILLUSTRATIVE EXAMPLE IN WHICH $T_\alpha < 0$

The previous discussion demonstrated that the hydrogen spin temperature can become negative in the presence of a large flux of Ly α photons that are primarily in the blue wing of the line. Here, we show a simple example of such a scenario. This example illustrates the relevant physical conditions to make $T_\alpha < 0$ and discusses the possible duration of this phenomenon. A Ly α point source is embedded in a neutral gas cloud that is contracting with a uniform velocity, v_i . The Ly α source is turned on at $t = 0$. The intrinsic Ly α

⁵ This equilibrium value is reached on a timescale of $\sim P_\alpha^{-1}$, provided Ly α scattering is the dominant level-mixing process.

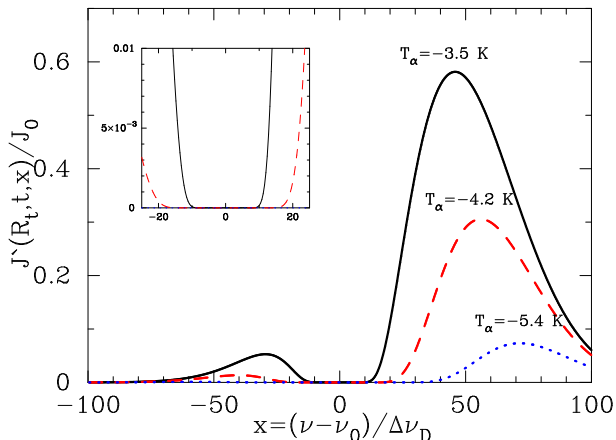


Figure 1. Three examples of Ly α spectra with a negative color temperature. These spectra were obtained after suppressing a blueshifted Gaussian emission line by a factor of $e^{-\tau_0 \phi(x)}$, with $\tau_0 = 10^5$ (black solid line), $\tau_0 = 10^{5.3}$ (red dashed line) and $\tau_0 = 10^6$ (blue dotted line, see text for more details). None of the spectra contain photons in the core of the line profile (which is shown better in the inset, which zooms on the spectra in the line core), and the majority of the photons lies blueward of the line center. The Ly α color temperature associated with each curve is labeled.

spectrum, expressed in the dimensionless frequency variable x , is Gaussian with a standard deviation of x_c . In the frame of the infalling gas this line appears blue shifted. The spectrum at the photon front, $R_t = ct$, becomes

$$J'(R_t, t, x) = J_0 e^{-\frac{(x-x_i)^2}{2x_c^2}} \times e^{-\tau_0 \phi(x)}, \quad (11)$$

where $x_i = v_i/v_{\text{th}}$, J_0 is arbitrary and $\tau_0 = \sigma_0 n_H R_t$. For large values of τ_0 , the spectrum at R_t practically only contains photons in the wing of the line, the majority of which lies blueward of the line center. This is shown in Figure 1 which shows $J'(R_t, t, x)$ for $\log[\tau_0] = 5.0$ (solid line); 5.3 (red dashed line) and 6.0 (blue dotted line), where $x_c = x_i = 30$ and the gas temperature, $T_{\text{gas}} = 10$ K. The color temperature (Eq. 7) associated with each curve is -3.5 , -4.2 and -5.5 K, respectively.

The color temperature remains negative only for a finite amount of time. The moment the core photons reach a given radius R , $T_\alpha \rightarrow T_{\text{gas}}$. The duration of time over which the color temperature remains negative determines whether the Ly α photons can establish population inversion in the hyperfine levels. It is difficult to analytically estimate by how much the core photons are delayed in their arrival at a given radius R . Resonant scattering causes a Ly α photon to undergo a random walk in frequency, which causes its mean free path to change during its random walk through space (Adams 1972; Loeb & Rybicki 1999). One consequence of this is that the average number of times a Ly α photon scatters to traverse a line center optical depth τ_0 scales as $\propto \tau_0$, as opposed to the $\propto \tau_0^2$ scaling expected for a standard random walk (Adams 1972; Harrington 1973; Neufeld 1990). The vast majority of these scattering events takes place in the line core, but spatial diffusion occurs predominantly in the line wings. The first Ly α photons that were emitted by the source in the line core to arrive at a radius R , are therefore mostly in the line wings. Similarly, frequency diffusion may cause Ly α

photons that were emitted by the source in the line wing, to emerge at radius R in the line core. To properly account for these effects, the precise duration of this negative color temperature episode should be determined with a Monte-Carlo code (see § 6, in which we give an example in which the color temperature, in fact, stays negative indefinitely). The previous discussion was meant to illustrate that a negative Ly α color temperature may (temporarily) be associated with the collapse of neutral gas clouds surrounding a central Ly α source that has just switched on.

5 SOURCE REQUIREMENTS

A key requirement for a negative hydrogen spin temperature is the absence of Ly α photons in the line center, as these would scatter and rapidly rearrange the level populations in the hyperfine transition such that $T_s \rightarrow T_{\text{gas}}$. So far, our calculation assumed that all Ly α photons were emitted by the central source and that the Ly α core photons are delayed in their arrival at a given radius, as their significantly shorter mean free path reduces their spatial diffusivity. However, Ly α core photons may emerge at a certain location through different channels. These are discussed in turn in the following subsections.

5.1 Ly α Production following Photoionisation

When hydrogen recombines after being photoionised by x-rays that managed to penetrate the neutral gas (collisional ionization at low temperatures is negligible), a Ly α photon is produced with a probability of $\sim 2/3$ (for case B recombination). The emergent Ly α photon has a high probability of being injected close to the line center. This effect is probably not important because the recombination time $t_{\text{rec}} = 1/(n_e \alpha) \gg t_{\text{cross}}$, particularly in an almost completely neutral medium (regardless of the gas temperature). A more important effect however, is that photoionisation by x-rays may produce energetic electrons that excite the $n = 2$ level of atomic hydrogen, which immediately results in the emission of a Ly α core photon (e.g. Chen & Miralda-Escude 2006). A way around the negative impact of x-rays is discussed in § 5.3, below.

5.2 Ly α Production through Cascades

Photons in the energy range $E = 10.2 - 13.6$ eV (hereafter ‘soft UV-photons’) can generally easily penetrate deep into a neutral medium, where they are absorbed by neutral hydrogen atoms, where they are excited by these soft UV photons, cascade down to their electronic ground state, during which there is a $\sim 35\%$ probability that a Ly α photon is emitted. Again, this Ly α photon is likely in the line core. It is shown below that this Ly α production mechanism has the potential to strongly suppress the existence of masers.

Consider the example discussed in § 4, but assume that the central source is also emitting soft UV photons. Ly α photons with $|x| \gtrsim 40$ can reach the radius corresponding to $\log[\tau_0] = 5.3$, without being scattered (for these photons $\tau < 1$). However, the same applies to Ly γ photons with

$|x_\gamma| \gtrsim 5$; Ly δ photons with $|x_\delta| \gtrsim 3$, etc.⁶ To obtain these numbers, we derived the cross-sections for higher-order Lyman-series transitions in Appendix B. Whereas the Ly α wing photons have a negligible probability of being scattered into the line center, the higher-order Lyman-series photons have a $\sim 35\%/5 = 7\%$ probability of being converted on the spot into a Ly α photon that is in the line core. The factor of 5 reflect that a higher order Lyman-series photon scatters on average ~ 5 times before undergoing a cascade (which results in a Ly α photon $\sim 35\%$ of the time, see Pritchard & Furlanetto 2005). These newly produced Ly α -core photons interact strongly with the neutral gas, causing their color temperature to approach the gas temperature. The evolution of the hydrogen spin temperature depends on which population of Ly α photons dominates the scattering rate. If the scattering rate of the disguised (or converted) Ly α photons dominates over that of the Ly α wing photons, then the hydrogen spin temperature is set by the color temperature of these converted Ly α photons.

The scattering rate of the converted Ly α photons can be written as

$$P_{\alpha,\text{con}} = \langle N \rangle \epsilon P_n = \langle N \rangle 4\pi \epsilon \int_{\text{Ly}\gamma}^{\text{Ly}\epsilon} \frac{J(\nu)}{h\nu} \sigma_{\text{tot}}(\nu) e^{-\tau(\nu)} d\nu. \quad (12)$$

Here, $\epsilon = 0.07$ is the mean probability for a Ly- n photon to be converted per scattering (Pritchard & Furlanetto 2005). P_n is the scattering rate of the higher-order Lyman-series photons. The optical depth $\tau(\nu) = N_H \sigma_{\text{tot}}(\nu)$, in which $N_H = 10^{17} \text{ cm}^{-2}$ is the total column density of intervening hydrogen (that corresponds to $\log[\tau_0] = 5.3$ at $T_{\text{gas}} = 10 \text{ K}$) and $\sigma_{\text{tot}}(\nu)$ is the absorption cross-section at frequency ν , obtained by summing over all Lyman-series transitions (derived in Appendix B). As mentioned earlier, a Ly β photon cannot be converted into a Ly α photon and so the integral is performed over $h\nu \in [12.8 - 13.6] \text{ eV}$. Furthermore, $\langle N \rangle$ is the average number of times a core photon scatters in the core before it disappears. This number is large and quite uncertain; we show below that $\langle N \rangle = 10^7$ provides a reasonable choice for its value.

To estimate $\langle N \rangle$, we first observe that it takes on average $\sim 10^4 - 10^5$ scattering events for a Ly α core photon to be scattered into the wing, $|x| > x_t \sim 3$ (Hummer 1962). However, photons close to the core-wing transition frequency, $|x_t|$, can scatter back into the line core in a single scattering event. Therefore, $\langle N \rangle$ should be higher. Velocity gradients present in more realistic models (than that discussed in § 4) of collapsing gas clouds facilitate the escape of Ly α photons. In the presence of velocity gradients the majority of the scattering events of a photon occur around its resonant region. For a *static* medium, a Ly α photon scatters on average $\sim \tau_0$ times to traverse an optical depth τ_0 (Adams 1972; Harrington 1973). The total optical depth of the resonant region, τ_{res} , can be calculated from the total optical depth over the scale for which the velocity changes by a thermal width (also known as the Sobolev

length), v_{th} : $\tau_{\text{res}} = n_H \sigma_0 v_{\text{th}} [dv_{\text{infall}}/dr]^{-1}$. If we approximate $dv_{\text{infall}}/dr \sim v_{\text{circ}}/r_{\text{vir}}$, where v_{circ} and r_{vir} are the circular velocity and virial radius of the host dark matter halo, then $\tau_{\text{res}} \sim 2 \times 10^6 [(1 + \delta)/60] [(1 + z_{\text{vir}})/9]^{3/2}$. Here, δ is the overdensity of the gas. Note that the temperature dependence has cancelled out in this expression. Therefore, for a photon to escape from its local resonant region, it scatters on average $\langle N \rangle \sim \tau_{\text{res}} \sim 10^6 - 10^7$ times.

Next we estimate the scattering rate of the Ly α wing photons (with a negative color temperature) using Eq. (9), where the flux density of Ly α wing photons is given by Eq. (11). Assuming the continuum is spectrally flat, i.e. $J(\nu)$ is independent of ν for $h\nu \in [10.2 - 13.6] \text{ eV}$, the ratio of $P_{\alpha,\text{con}}$ and P_α is given by

$$P_{\alpha,\text{con}}/P_\alpha \sim \langle N \rangle / J_0, \quad (13)$$

where J_0 is the amplitude of the Ly α emission line (as in Eq. (11), or more accurately, the ratio of the peak Ly α to the continuum flux density). Of course, this approximation depends on the assumed value of N_H and width of the intrinsic Ly α emission line, x_c . However, we have found the dependence on these parameters to be rather weak. According to Eq. (13), the converted Ly α photons dominate the scattering rate, unless $J_0 > \langle N \rangle$, i.e. the intrinsic peak Ly α flux density must lie a factor of $\langle N \rangle \sim 10^7$ above the continuum. It is more common to express the prominence of the Ly α line through its equivalent width (EW). In this example, $\text{EW} = 0.1 J_0 \text{ \AA}$. Therefore, unless $\text{EW} > 0.1 \langle N \rangle \sim 10^6 \text{ \AA}$, the Ly α scattering rate is determined by the converted Ly α photons and will drive the spin temperature to its color temperature (which is not negative). An intrinsic Ly α EW of 10^6 \AA is exceptionally high, several orders of magnitude above the values that are typically observed in $z = 6.5$ galaxies (Rhoads et al. 2004; Shimasaku et al. 2006). In § 5.3 below, we explore mechanisms which can remove the soft UV-photons while transmitting the Ly α photons.

5.3 Blocking Soft UV & x-ray Photons with a Multi-Phase Interstellar Medium

The discussion of § 5.2 showed that in order for Maser conditions to prevail, the flux of soft UV photons must be reduced substantially. A sufficiently large column of atomic hydrogen $N_H \gtrsim 10^{23.5} \text{ cm}^{-2}$ is opaque to all soft UV-photons, while it could theoretically transmit Ly α photons. However, as shown in Appendix C, the Ly α photons emerging from a thick obscuring slab of neutral atomic hydrogen cannot produce maser conditions. In this section, we discuss a more promising mechanism.

It has been shown that a multiphase interstellar medium (ISM) can transmit a significantly larger fraction of Ly α photons compared to continuum photons (Neufeld 1991; Hansen & Oh 2006). These circumstances have been invoked to explain the large escape fraction of Ly α photons from galaxies which show strong evidence of containing large amounts of dust. It can also be invoked to explain the observation that high redshift galaxies often have Ly α equivalent widths exceeding the value which is believed to be theoretically plausible for a normal stellar population. In this model, the ISM consists of cold, dense, dusty clumps embedded in a hot medium. The Ly α scatters off the cold clumps and propagates mainly through the hot, dust free, interclump

⁶ Ly β photons can be ignored here since these have a zero probability of being transformed into Ly α (Pritchard & Furlanetto 2005).

medium. The continuum photons, on the other hand, can easily penetrate the clumps where it is subject to absorption by dust. The exact ratio of the Ly α transmission, f_α , and the continuum transmission, f_c depends on details such as (i) the hydrogen column density of individual clumps, (ii) the dust content of clumps, (iii) the covering factor of the clumps, (iv) the number of clumps (Hansen & Oh 2006). Clearly, a systematic exploration of all these parameters is beyond the scope of this paper. Here, we describe the general requirements to severely suppress the continuum, while transmitting a large fraction of the Ly α photons.

To destroy a large fraction of the continuum requires a large total column of dust. The total continuum suppression can be estimated from $\langle e^{-\tau_d} \rangle$, where $\tau_d = N_H \epsilon_d \sigma_d$, in which N_H is the total column of hydrogen of a clump, σ_d is the dust cross section per hydrogen nuclei and ϵ_d is the probability that a continuum photon is absorbed (rather than scattered). For the diffuse HI phase of the Milky Way, $\tau_d = 0.5(N_H/10^{21} \text{ cm}^2)$ (Hansen & Oh 2006, and references therein), which indicates that to get $\tau_d \gtrsim 12$ (corresponding to $\langle e^{-\tau_d} \rangle \lesssim 10^{-5}$) requires $N_H \gtrsim 3 \times 10^{22} \text{ cm}^{-2}$, provided these clumps have the same dust content. We point out that local starburst galaxies may have gas surface density well in excess of this value (see e.g. Fig 2 of Thompson et al. 2006), with columns reaching values $\gtrsim 10^{24} \text{ cm}^{-2}$. Of course, high redshift galaxies are expected to be less massive, but if we approximate the gas surface density as $\Sigma_{\text{gas}} \propto M_{\text{gas}}/R_{\text{gas}}^2 \propto M_{\text{halo}}/R_{\text{vir}}^2 \propto M_{\text{halo}}^{1/3} (1+z_{\text{vir}})^2$, then we find that systems with masses lower by a factor of 10^3 that virialized at $z \gtrsim 6$ (vs. $z \sim 1$ for local starburst galaxies), may possess comparable or bigger gas surface densities.

This total column of dust and hydrogen can reside either in a large number of small clumps, or a small number of large clumps. As is shown by Hansen & Oh (2006, their Fig. 18), the ratio f_α/f_c decreases with the total number of times that a Ly α photon scatters. In order to maximise the ratio f_α/f_c , we therefore need to minimise the number of times a Ly α photon scatters, which is achieved by maximising the clump size. If these clumps can suppress the continuum by a factor $\gtrsim 10^5$, then intrinsic Ly α equivalent widths exceeding EW $\gtrsim 10^2 \text{ \AA}$ are required to allow for $T_\alpha < 0$, which is a much less stringent requirement than that obtained in § 5.2. The presence of a large column of gas, $N_H \gtrsim 3 \times 10^{22} \text{ cm}^{-2}$, would also attenuate the x-ray flux emitted by the galaxy (especially when the gas has a large dust content) enough to allow $T_\alpha < 0$. This point is further quantified in § 6.

The discussion below focuses on the resulting hypothetical situation in which sources exist in the high redshift universe, that allow a significant fraction of their Ly α to be transmitted, while their continuum flux is suppressed by a factor $\gtrsim 10^5$.

6 SIMULATING A BRIGHT LY α SOURCE IN A COLLAPSING CLOUD OF NEUTRAL GAS

6.1 The Simulation

We use the Monte-Carlo code described in Dijkstra et al. (2006) for our radiative transfer calculation. This code calculates the Ly α transfer through spherically symmetric gas clouds, with arbitrary density and velocity fields. The de-

tailed micro-physics of Ly α scattering (e.g. energy loss due to atomic recoil) is incorporated in this code. For details and descriptions of tests performed on the code, the interested reader is referred to the above paper. The code was expanded for the work presented in this paper to follow the time evolution of the Ly α radiation field as a function of position. This was achieved by keeping track of the total time that elapsed since a Ly α photon was emitted. When this time reaches user-specified values, a 'snapshot' of the photon trajectory is taken and its location and frequency in the frame of the infalling gas is recorded.

The bright Ly α source is embedded in a neutral collapsing gas cloud. The total (dark matter + baryons) mass of the halo hosting the collapsing cloud is $M_{\text{tot}} = 10^{11} M_\odot$. Collapse occurs at redshift $z = 8$. Here, we use a more realistic gas density and velocity field compared to that of § 4. Within the virial radius, $r_{\text{vir}} = 16 \text{ kpc}$ the gas density is assumed to trace the dark matter (which is given by a NFW profile with concentration parameter $c = 5$) modified by a core at $r < 3r_s/4$ (see Maller & Bullock 2004, their Eq. 9-11) where $r_s = r_{\text{vir}}/c$. The infall velocity field, $v(r)$, is assumed to be linear with $v(r) = -v_{\text{circ}}[r/r_{\text{vir}}]$ in which $v_{\text{circ}} (= 158 \text{ km s}^{-1})$ is the circular velocity of the host dark matter halo. Beyond the virial radius, $r > r_{\text{vir}}$, infall of gas continues and we adopt the density and velocity profiles based on the curves shown in Figures 2 and 4 of Barkana (2004; see Dijkstra et al, 2006, for a more detailed discussion of this choice). The gas collapsing outside the galaxy is assumed to be cold, $T_{\text{gas}} = 300 \text{ K}$. Recent calculations by Birnboim & Dekel (2003) have shown that virial shocks are likely not to exist in objects with masses below $M_{\text{tot}} \sim 2 \times 10^{11} M_\odot$ (also see Kereš et al. 2005). Our choice of T_{gas} then represents the minimum temperature that can be reached through cooling by H $_2$ molecules.

Photons are injected at $t = 0$ following a Gaussian frequency distribution with $\sigma_v = v_{\text{circ}}$. Snapshots were taken of the Ly α frequency distribution at $r_{\text{sn}} = 5, 10, 15$ and 20 kpc at four different times: $t = 4t_{\text{cross}}$, $t = 6t_{\text{cross}}$, $t = 8t_{\text{cross}}$ and $t = 10t_{\text{cross}}$, where $t_{\text{cross}} \equiv r_{\text{sn}}/c$ is the light-crossing time to radius r_{sn} . The spectra derived from these snapshots at $r = 15 \text{ kpc}$ are shown in Figure 2 as the *black* ($t = 4t_{\text{cross}}$) and *red* ($t = 10t_{\text{cross}}$) histogram. The Ly α photons lie systematically to the blue side of the line, by amounts greatly exceeding the infall velocity. The inset of the Figure zooms on the line core and shows more clearly that no photons are present in the core of the line profile. The reason for the large shift to the blue side of the line can be easily understood: as the Ly α photons propagate outward through an optically thick collapsing gas cloud, energy is transferred from the gas to the photons, which results in an overall blueshift of the line (Zheng & Miralda-Escudé 2002; Dijkstra et al. 2006), which can exceed the infall velocity of the infalling gas significantly (Large velocity shifts are common in Ly α radiative transfer through optically thick gas clouds. In order for Ly α to escape from an optically very thick gas cloud, the photons need to diffuse far into the line wings, where the gas cloud becomes optically thinner.).

Each subsequent timestep the Ly α line shifts slightly further to the blue and broadens. This broadening of the line can be thought of as being a direct consequence of the frequency diffusion associated with Ly α scattering. This dif-

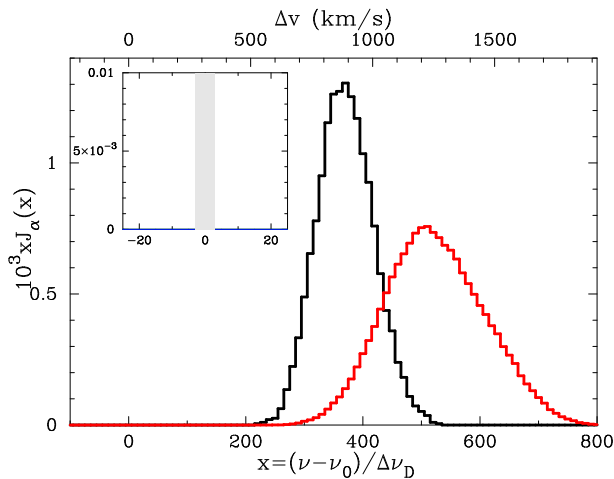


Figure 2. Time evolution of the Ly α spectrum 'seen' by a gas element at $r = 15$ kpc, inside a collapsing cloud of neutral hydrogen. The Ly α radiative transfer was calculated using a Monte Carlo code. All Ly α photons are inserted at $t = 0$, and the spectra are shown at $t = 4t_{\text{cross}}$ (black) and $t = 10t_{\text{cross}}$ (red), where $t_{\text{cross}} \equiv r_{\text{sn}}/c$ is the light-crossing time to radius $r_{\text{sn}} = 15$ kpc. All spectra are systematically blueshifted relative to the line center, which is due to energy transfer from the infalling gas to the Ly α photons. These distributions of Ly α photons have $T_\alpha \sim -160$ K ($t = 4t_{\text{cross}}$) and $T_\alpha \sim -230$ K ($t = 10t_{\text{cross}}$). For $P_\alpha \gtrsim 5 - 7 \times 10^{-11} \text{ s}^{-1}$, $T_s < 0$.

fusion process in a collapsing cloud has a preference of shifting the photons further to the blue.

It is interesting to note that the core photons do not emerge at all at $r = 15$ kpc (and at all radii $r > 5$ kpc). In § 4 we argued that core photons would eventually arrive at any radius, causing T_α to become positive. This argument did not take into account, however, that energy is transferred from the gas to the Ly α photons as they are propagating outward through the neutral collapsing gas cloud, causing an overall blueshift. Therefore, the color temperature of the Ly α photons emitted by the source stays negative for the entire lifetime of the Ly α source. We point out that for continuous Ly α emission, the Ly α spectrum at a given radius is some average of the spectra calculated above.

6.2 The Ly α Color Temperature and Hydrogen Spin Temperature

The Ly α color temperature associated with the four spectra of Figure 2 is $T_\alpha = -160$ K at $t = 4t_{\text{cross}}$ and $T_\alpha = -230$ K at $t = 10t_{\text{cross}}$. For these color temperatures, T_s is negative when the Ly α scattering rate $P_\alpha \gtrsim 5 - 7 \times 10^{-11} \text{ s}^{-1}$ (§ 3.2). For the spectra shown in Figure 2, Ly α luminosities exceeding a few times $10^{45} \text{ erg s}^{-1}$ are required to produce $P_\alpha \gtrsim 5 - 7 \times 10^{-11} \text{ s}^{-1}$ at $r = 10 - 15$ kpc (Eq. 9). To produce such high Ly α luminosities with stars requires a high star formation rate. The Ly α luminosity can be estimated as $L_{\text{Ly}\alpha} \sim 10^{42} (\dot{M}/M_\odot \text{ yr}^{-1}) \text{ erg s}^{-1}$, where \dot{M} is the star formation rate (e.g. Loeb et al. 2005). According to this relation, $L_{\text{Ly}\alpha} \gtrsim 10^{45} \text{ erg s}^{-1}$ requires $\dot{M} \gtrsim 10^3 M_\odot/\text{yr}$. Note that this relation assumes that stars form according to the conventional Salpeter mass function. For a top-heavy mass

function of stars, the Ly α luminosity may be higher by an order of magnitude (Schaerer 2003).

We point out that the scattering rate of Ly α core photons produced by x-ray photons is smaller than the Ly α wing-scattering rate. The x-ray luminosity, L_X , of a galaxy can be similarly related to its star formation rate through $L_X \sim 10^{40} (\dot{M}/M_\odot \text{ yr}^{-1}) \text{ erg s}^{-1}$ (e.g. Furlanetto 2006). The Ly α core scattering rate is estimated from

$$P_{X \rightarrow \alpha} = 4\pi \langle N \rangle \int \frac{f_X(\nu)}{h\nu} \sigma(\nu) e^{-\tau_X(\nu)} d\nu, \quad (14)$$

where $f_X(\nu) \propto \nu^{-1.5}$ and $\int_{0.2 \text{ keV}}^{\infty} f_X(\nu) d\nu = L_X$ (see Furlanetto 2006, and references therein). Furthermore, $\tau_X(\nu) = N_H b_m \sigma_H(\nu)$, in which $N_H = 3 \times 10^{22} \text{ cm}^{-2}$ (§ 5.3), σ_H is the photoionisation cross section of hydrogen and $b_m \sim 6$ is the boost in this cross-section due to the presence of metals (Dijkstra et al. 2005, their Eq. 1). Numerically, we find that $P_{X \rightarrow \alpha} \sim 10^{-13} \text{ s}^{-1}$ at $r = 15$ kpc. Therefore, core-photon scattering is subdominant relative to the Ly α wing scattering and the Ly α wing photons with negative T_α dominate the scattering rate, causing T_s to become negative.

6.3 The Gain of the Maser

Now that we have established a scenario in which in the spin temperature is negative, we estimate the masers gain factor. The Ly α transfer code provides us with Ly α spectra at $r = 5, 10, 15$ and 20 kpc. We calculate T_α at each radius, ignoring for simplicity the slight variation in T_α with time, and use Eq. (8) to calculate T_s at these radii. We note that $T_s \sim T_\alpha$ if P_α (and therefore $L_{\text{Ly}\alpha}$) is increased by a factor of 3 relative to the values quoted above. The length scale that is relevant to calculate the total gain is given by the Sobolov length, ℓ_S , which is the length over which the velocity changes by less than the thermal velocity, $\ell_S = v_{\text{th}}/[dv(r)/dr]$. For the example calculated above, $\ell_S = v_{\text{th}} R_{\text{vir}}/v_{\text{circ}} = 0.014 (T_{\text{gas}}/300\text{K})^{1/2} R_{\text{vir}}$. The total gain γ is then estimated from the product $\ell_S \times \alpha$, in which α is given by Eq. (4). We find that $\gamma = 3 \times 10^{-3} (|T_s|/200\text{K})^{-1} (1 + \delta)/40$, which is independent of the gas temperature. Since the total maser amplification is given by $e^\gamma \sim 1.003 (|T_s|/200\text{K})^{-1}$, this does not provide a dramatic effect.

To get a larger gain of the maser we need a larger Sobolov length ℓ_S , which can be obtained for a different infall velocity field $v(r)$. In particular, for decelerating inflows with $dv/dr < 0$ one may construct velocity fields that give an arbitrarily long Sobolov length (Rybicki & Hummer 1978).⁷ Although this requires some fine tuning, the gain factor can be considerably larger than the value quoted above.

Another way of obtaining a larger gain factor is when coherent clumps of gas, such as mini-halos (defined as objects with a virial temperature below the hydrogen cooling threshold $T_{\text{vir}} < 10^4$ K), are present in the infalling gas. In the absence of molecules (which can easily be dissociated by an extragalactic background of Lyman Werner photons, see e.g. Wyithe & Cen 2006 and references therein) gas that

⁷ For example, a velocity field of the form $v(r) = -r/\sqrt{r^2 - l^2}$, for $r > l$, gives an infinitely large Sobolov length at impact parameter l .

resides in a collapsing mini-halo, gets shocked to the virial temperature of its host halo, T_{vir} , and is unable to cool to lower temperatures. Therefore, star formation does not occur and one is left with a gravitationally-bound gas cloud. The total column of hydrogen through mini-halos is typically $N_H = 10^{20} - 10^{21} \text{ cm}^{-2}$. Ly α photons blueshifted by more than $v \gtrsim (a\tau_0)^{1/3} v_{\text{th}} = 200 - 400 (T_{\text{gas}}/10^4)^{1/6} \text{ km s}^{-1}$, can propagate through these clouds without being scattered in the line core, as required for the Ly α color temperature to remain negative inside the mini-halo. Since the spectra shown in Figure 2 satisfy this requirement, it seems possible for the population of Ly α photons shown in Figure 2 to cause population inversion in the mini-halo gas.

Furlanetto et al. (2006) give the line-center optical depth τ to 21-cm radiation through the center of the mini-halo, $\tau \sim 0.026[(1+z)/10]^{1/2} (M_{\text{tot}}/10^7 M_\odot)^{-2/3}$. This τ is related to our gain factor, γ , via $\gamma = \tau \bar{T}_{\text{gas}}/|T_s|$, in which $\bar{T}_{\text{gas}} \sim T_{\text{vir}}$ is the mean temperature of the virialised gas in the mini-halo. We therefore obtain $\gamma = 0.5[(1+z)/10]^{1/2}$. The factor e^γ increases dramatically for denser mini-halos that collapsed at higher redshift (as long as collisional excitation of the 21-cm line inside these denser mini-halos does not bring T_s towards T_{gas}), and for lower values of $|T_s|$. For $\gamma \gtrsim 4.6$ the 21cm flux from the CMB is amplified by a factor of $e^\gamma \gtrsim 100$ (see Eq. 4). This magnification would amount to a brightness temperature $T_b \sim 100(\lambda_s^2/2k) I_{\text{CMB}} \sim 100 \times T_{\text{CMB},0} = 270 \text{ K}$.

7 CONCLUSIONS

We have examined whether the Wouthuysen-Field effect can cause population inversion in the hyperfine levels of atomic hydrogen. The accompanying stimulated 21-cm emission could boost the 21-cm Epoch of Reionisation signal by orders of magnitude.

We have derived an expression for the Ly α color temperature T_α for arbitrary frequency distributions of Ly α photons (Eq. 7). We used this expression to show that T_α is negative for a population of Ly α photons which are in the blue wing of the line profile, as may be the case for Ly α photons emitted by a bright source embedded within a collapsing cloud of neutral hydrogen (§ 4 and § 6).

A key requirement for having $T_\alpha < 0$ is the absence of Ly α photons in the line center, as these would scatter and rapidly rearrange the level populations in the hyperfine transition such that $T_s \rightarrow T_{\text{gas}}$. If all Ly α photons are emitted by the central source, then Ly α core photons are delayed in their arrival at a given radius, as their significantly shorter mean free path reduces their spatial diffusivity. We discussed in § 5, however, that Ly α core photons can show up at a given location through two different channels. Photoionisation by x-rays that penetrate the neutral gas can produce energetic electrons which can excite the $n = 2$ level of atomic hydrogen, which immediately results in the emission of a Ly α core photon (§ 5.1). Furthermore, a relatively low flux of photons with energies $E \in [10.2 - 13.6] \text{ eV}$ (referred to as 'soft UV' or Lyman-Werner photons) may almost instantly insert enough Ly α core photons to cause $T_\alpha \rightarrow T_{\text{gas}}$ (§ 5.2). In § 5.3, we specified conditions in a clumpy, two-phase interstellar medium (ISM), in which cold, dusty clumps with columns of gas exceeding $3 \times 10^{22} \text{ cm}^{-2}$ suppress the con-

tinuum flux by a factor of $\gtrsim 10^5$, while the Ly α can mostly be transmitted through the hot, ionised interclump medium. These extreme conditions are essential for allowing the possibility of a negative Ly α color (and hydrogen spin) temperature.

Finally, we showed in § 6 that if sources with a strongly suppressed continuum (e.g. through the two-phase ISM) exist, then in order for the hydrogen spin temperature to reach negative values and result in a 21-cm maser, large Ly α luminosities are required, $L_{\text{Ly}\alpha} \gtrsim 10^{45} \text{ erg s}^{-1}$. Ly α luminosities of this magnitude are reached when the star formation rate $\dot{M} \gtrsim 10^3 M_\odot/\text{yr}$. If the high redshift ($z \gtrsim 6$) universe contains starburst galaxies with these extreme properties, then 21-cm masers exist in the cold infalling gas around these galaxies. The total associated maser amplification could be substantial for mini-halos.

We therefore conclude that if the high redshift ($z \gtrsim 6$) universe contains starburst galaxies with these extreme properties, then 21-cm masers may exist in the cold infalling mini-halos around these galaxies. Conversely, if anomalously high 21-cm fluxes are found at high redshifts by forthcoming low-frequency observatories, then this would be indicative of sources with the above-mentioned properties.

Acknowledgments We thank George Rybicki and Stuart Wyithe for useful discussions. MD would like to thank Harvard's Institute for Theory & Computation for its hospitality. MD is supported by the Australian Research Council. AL was supported in part by NASA grants NAG 5-1329 and NNG05GH54G.

REFERENCES

- Adams, T. F. 1972, *ApJ*, 174, 439
 Birnboim, Y., & Dekel, A. 2003, *MNRAS*, 345, 349
 Chen, X., & Miralda-Escudé, J. 2004, *ApJ*, 602, 1
 Chen, X., & Miralda-Escudé, J. 2006, submitted to *ApJ*, astro-ph/0605439
 Dijkstra, M., Haiman, Z., & Scharf, C. 2005, *ApJ*, 624, 85
 Dijkstra, M., Haiman, Z., & Spaans, M. 2006, Accepted for publication in *ApJ*, astro-ph/0510407
 Fan, X., et al. 2006, *AJ*, 132, 117
 Field, G. B. 1959, *ApJ*, 129, 551
 Furlanetto, S. R., & Loeb, A. 2002, *ApJ*, 579, 1
 Furlanetto, S. R., & Loeb, A. 2004, *ApJ*, 611, 642
 Furlanetto, S. 2006, submitted to *MNRAS*, astro-ph/0604040
 Furlanetto, S., Oh, S. P., & Briggs, F. 2006, accepted by *Physics Reports*, astro-ph/0608032
 Hansen, M., & Oh, S. P. 2006, *MNRAS*, 367, 979
 Harrington, J. P. 1973, *MNRAS*, 162, 43
 Hirata, C. M. 2006, *MNRAS*, 367, 259
 Hummer, D. G. 1962, *MNRAS*, 125, 21
 Iliiev, I. T., Shapiro, P. R., Ferrara, A., & Martel, H. 2002, *ApJL*, 572, L123
 Kaplan, S. A., Kleinman, E. B., & Oiringel, I. M. 1979, *Soviet Astronomy Letters*, 5, 184
 Kashikawa, N., et al. 2006, to appear in *ApJ*, astro-ph/0604149
 Kereš, D., Katz, N., Weinberg, D. H., & Davé, R. 2005, *MNRAS*, 363, 2
 Loeb, A., & Rybicki, G. B. 1999, *ApJ*, 524, 527

- Loeb, A., & Zaldarriaga, M. 2004, *Physical Review Letters*, 92, 211301
- Loeb, A., Barkana, R., & Hernquist, L. 2005, *ApJ*, 620, 553
- Madau, P., Meiksin, A., & Rees, M. J. 1997, *ApJ*, 475, 429
- Maller, A. H., & Bullock, J. S. 2004, *MNRAS*, 355, 694
- Meiksin, A. 2000, in *Perspectives on Radio Astronomy*, Published by ASTRON. ISBN: 90-805434-1-1, 340 pages, 2000, p.37, 37–+
- Meiksin, A. 2006, *MNRAS* submitted, astro-ph/0603855
- Menzel, D. H., & Pekeris, C. L. 1935, *MNRAS*, 96, 77
- Neufeld, D. A. 1990, *ApJ*, 350, 216
- Neufeld, D. A. 1991, *ApJL*, 370, L85
- Osterbrock, D. E. 1962, *ApJ*, 135, 195
- Peebles, P. J. E. 1993, *Princeton Series in Physics*, Princeton, NJ: Princeton University Press, —c1993,
- Peterson, J. B., Pen, U., & Wu, X. 2006, *Astronomical Society of the Pacific Conference Series*, 345, 441
- Pritchard, J. R., & Furlanetto, S. R. 2005
- Pritchard, J. R., & Furlanetto, S. R. 2006, submitted to *MNRAS*, astro-ph/0607234
- Rhoads, J. E., et al. 2004, *ApJ*, 611, 59
- Rybicki, G. B., & Hummer, D. G. 1978, *ApJ*, 219, 654
- Rybicki, G. B., & Lightman, A. P. 1979, *Radiative processes in astrophysics* (New York, Wiley-Interscience, 1979. 393 p.)
- Schaerer, D. 2003, *A&A*, 397, 527
- Scott, D., & Rees, M. J. 1990, *MNRAS*, 247, 510
- Shimasaku, K., et al. 2006, *PASJ*, 58, 313
- Spaans, M., & Silk, J. 2006, submitted to *ApJ*, astro-ph/0601714
- Spergel, D. N., et al. 2003, *ApJS*, 148, 175
- Thompson, T. A., et al. 2006, *ApJ*, 645, 186
- Venkatesan, A., Giroux, M. L., & Shull, J. M. 2001, *ApJ*, 563, 1
- Varshalovich, D. A. 1967, *Soviet Physics JETP*, 25, 157
- Wouthuysen, S. A. 1952, *AJ*, 57, 31
- Wyithe, S., & Cen, R. 2006, submitted to *ApJ*, astro-ph/0602503
- Zheng, Z., & Miralda-Escudé, J. 2002, *ApJ*, 578, 33
- Zygelman, B. 2006, in preparation

APPENDIX A: DERIVATION OF THE LY α COLOR TEMPERATURE**A1 The 3-Level Hydrogen Atom without Collisions and CMB photons**

In this section we derive the expression for the Ly α color temperature under the simplification that the hydrogen atom only consists of 3 levels: The 2 hyperfine levels in the electronic ground state, denoted by 1 and 2 as in the paper, and 1 level in the excited state (with statistical weight $g_3 = 3$. The final result of this calculation does not depend on g_3). The main goal of this calculation is that it simplifies, and illuminates, the analysis for the realistic 6-level hydrogen atom in Appendix A2.

The rate equation for the ground state reads (ignoring collisions+ scattering by CMB photons)

$$\frac{\partial n_1}{\partial t} = n_2 A_{21} - B_{13} \frac{A_{32}}{A_{32} + A_{31}} \bar{J} n_1 + B_{23} \frac{A_{31}}{A_{31} + A_{32}} \bar{J} n_2 \quad (\text{A1})$$

Substituting $n_2 = n_H - n_1$, $B_{13} = 3B_{31}$, $B_{23} = B_{32}$, $B_{ud} = A_{ud} \frac{c^2}{2h\nu_0^3}$ yields

$$\frac{\partial n_1}{\partial t} = (n_H - n_1) A_{21} - 3n_1 \bar{A} \frac{c^2}{2h\nu_0^3} \int J(\nu) \phi_{13}(\nu) d\nu + (n_H - n_1) \bar{A} \frac{c^2}{2h\nu_0^3} \int J(\nu) \phi_{23}(\nu) d\nu, \quad (\text{A2})$$

where $\phi(\nu)$ is the 'normalised line profile' (Rybicki & Lightman 1979) and $\bar{A} = \frac{A_{31} A_{32}}{A_{31} + A_{32}}$. Next assume that $\phi_{23}(\nu) = \phi_{13}(\nu + \Delta\nu_S) \approx \phi_{13}(\nu) + \Delta\nu_S \frac{\partial \phi_{13}}{\partial \nu}$, where $\Delta\nu_S = 1.42$ GHz. If we define

$$c_1 = \frac{1}{4} \bar{A} \frac{c^2}{2h\nu_0^3} \int \phi_{13}(\nu) J(\nu) d\nu; \quad c_2 = -\frac{1}{4} \bar{A} \frac{c^2}{2h\nu_0^3} \Delta\nu_S \int \frac{\partial \phi_{13}}{\partial \nu} J(\nu) d\nu, \quad (\text{A3})$$

then Eq. A2 can be rewritten as

$$\frac{\partial y}{\partial t} = (1 - y) A_{21} + c_1 - c_2 - y(4c_1 - c_2), \quad (\text{A4})$$

after dividing the left and right hand side by n_H and after defining $y = n_1/n_H$. The equilibrium value of y , obtained by setting $\partial y/\partial t=0$, is

$$y = \frac{A_{21} + c_1 - c_2}{A_{21} + 4c_1 - c_2} \approx \frac{c_1 - c_2}{4c_1 - c_2} \approx \frac{1}{4} - \frac{3}{16} \frac{c_2}{c_1}, \quad (\text{A5})$$

which corresponds to a spin temperature T_s of

$$T_s \approx \frac{3y}{4y - 1} T_* = -\frac{c_1}{c_2} T_* = \frac{\int \phi_{13}(\nu) J(\nu) d\nu}{\Delta\nu_S \int \frac{\partial \phi_{13}}{\partial \nu} J(\nu) d\nu} T_* \equiv T_\alpha. \quad (\text{A6})$$

Here the last definition only states that if Ly α scattering were the dominant process regulating the level populations in the 21 cm transition, then the equilibrium spin temperature is equal to the Ly α color temperature. Since $h\Delta\nu_S = kT_*$, this yields Eq. (7).

A2 The 6-Level Hydrogen Atom without Collisions and CMB photons

Here, the more general expression for the Ly α color temperature is derived, taking into account hyperfine splitting in the Hydrogen atom's $n = 1$ and $n = 2$ states, following Meiksin (2000) and Hirata (2006). Ignoring collisions and absorption and re-emission of CMB photons, the rate equation for atoms in the $n = 1$ state is

$$\begin{aligned} \frac{\partial n_1}{\partial t} &= n_2 A_{21} + \bar{J} \left[-B_{14} \frac{A_{42}}{A_{42} + A_{41}} n_1 + B_{24} \frac{A_{41}}{A_{41} + A_{42}} n_2 - B_{15} \frac{A_{52}}{A_{52} + A_{51}} n_1 + B_{25} \frac{A_{51}}{A_{51} + A_{52}} n_2 \right] = \\ &= n_2 A_{21} + \bar{J} \frac{c^2}{2h\nu_0^3} \left[-\frac{g_4}{g_1} \frac{A_{41} A_{42}}{A_{42} + A_{41}} n_1 + \frac{g_4}{g_2} \frac{A_{42} A_{41}}{A_{41} + A_{42}} n_2 - \frac{g_5}{g_1} \frac{A_{51} A_{52}}{A_{52} + A_{51}} n_1 + \frac{g_5}{g_2} \frac{A_{52} A_{51}}{A_{51} + A_{52}} n_2 \right] \end{aligned} \quad (\text{A7})$$

where we used the relations $B_{du} = \frac{g_u}{g_d} B_{ud} = \frac{g_u}{g_d} \frac{c^2}{2h\nu_0^3} A_{ud}$, and the notation $\bar{J} \equiv \int J(\nu) \phi(\nu) d\nu$. Following Meiksin (2000),

$$A_{41} = \frac{1}{3} A_\alpha, \quad A_{42} = \frac{2}{3} A_\alpha, \quad A_{51} = \frac{2}{3} A_\alpha, \quad A_{52} = \frac{1}{3} A_\alpha, \quad , \quad (\text{A8})$$

where $A_\alpha = 6.25 \times 10^8 \text{ s}^{-1}$, is the total Einstein A-coefficient, and $g_1 = 1$, $g_2 = 3$, $g_4 = 3$ and $g_5 = 3$. We get

$$\frac{\partial n_1}{\partial t} = n_2 A_{21} + \frac{c^2}{2h\nu_0^3} A_\alpha \left[-\frac{2}{3} n_1 \int J(\nu) \phi_{14}(\nu) d\nu + \frac{2}{9} n_2 \int J(\nu) \phi_{24}(\nu) d\nu - \frac{2}{3} n_1 \int J(\nu) \phi_{15}(\nu) d\nu + \frac{2}{9} n_2 \int J(\nu) \phi_{25}(\nu) d\nu \right]. \quad (\text{A9})$$

All line profiles are the same, apart from an offset in frequency: $\phi_{24}(\nu) = \phi_{14}(\nu + \Delta\nu_S)$, $\phi_{25}(\nu) = \phi_{15}(\nu + \Delta\nu_S)$ and $\phi_{14}(\nu) = \phi_{15}(\nu + \Delta\nu_G)$, where $\Delta\nu_G = 10.89$ GHz and $\Delta\nu_S = 1.42$ GHz (Hirata 2006). If we approximate $\phi(\nu + \Delta\nu) \approx \phi(\nu) + \Delta\nu \frac{\partial \phi}{\partial \nu}$ and write everything in terms of ϕ_{15} (which is written as $\phi(\nu)$ hereafter), and replace n_2 with $n_H - n_1$, we get

$$\frac{\partial n_1}{\partial t} = n_2 A_{21} + \frac{c^2}{9h\nu_0^3} A_\alpha \left[n_H \int J(\nu) \left(2\phi(\nu) + \frac{\partial \phi}{\partial \nu} \Delta\nu_G + 2 \frac{\partial \phi}{\partial \nu} \Delta\nu_S \right) d\nu - n_1 \int J(\nu) \left(8\phi(\nu) + 4 \frac{\partial \phi}{\partial \nu} \Delta\nu_G + 2 \frac{\partial \phi}{\partial \nu} \Delta\nu_S \right) d\nu \right]. \quad (\text{A10})$$

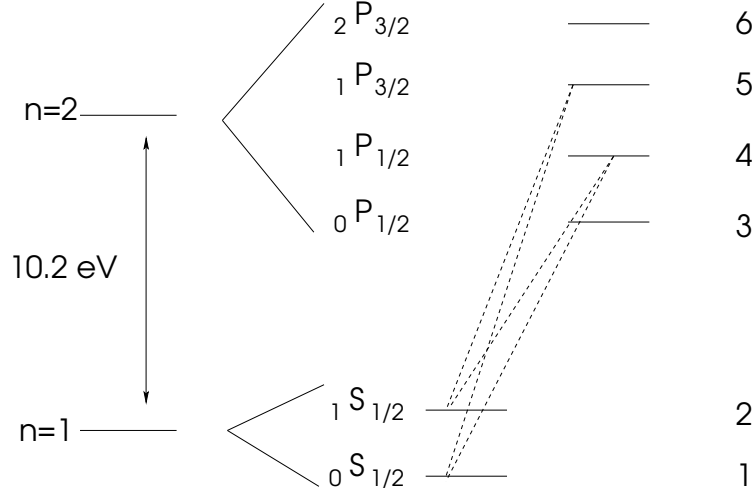


Figure A1. Schematic depiction of hyperfine splitting of the electronic ground state ($n=1$) and the first excited state ($n=2$) of the hydrogen atom. This 6-level model has been used to arrive at the expressions for the Ly α color temperature, Eq. A13 and the spin temperature, Eq. A16. The *dashed lines* denote the transitions involved in the mixing of hyperfine levels. Levels 3 and 6 do not contribute to the mixing of levels. The notation used for the individual levels is ${}_F L_J$, where L is the orbital angular momentum, J the total angular momentum quantum number. Here, F is the sum of J and I , the nuclear spin quantum number.

Following the procedure of Appendix A1, we write $y = n_1/n_H$ and get

$$\frac{\partial y}{\partial t} = (1-y)A_{21} + b_1 - b_2 - y(4b_1 - b_2) \quad (\text{A11})$$

in which

$$b_1 = A_\alpha \frac{c^2}{9h\nu_0^3} \int J(\nu) \left(2\phi(\nu) + \frac{\partial \phi}{\partial \nu} \Delta\nu_G \right) d\nu; \quad b_2 = -A_\alpha \frac{2c^2}{9h\nu_0^3} \Delta\nu_S \int \frac{\partial \phi}{\partial \nu} J(\nu) d\nu \quad (\text{A12})$$

Because Eq. A11 is equivalent to Eq. A4, the equilibrium spin temperature is simply

$$T_s = -\frac{b_1}{b_2} T_* = \left[\frac{\int \phi(\nu) J(\nu) d\nu}{\Delta\nu_S \int \frac{\partial \phi}{\partial \nu} J(\nu) d\nu} + \frac{\Delta\nu_G}{\Delta\nu_S} \right] T_* \approx \left[\frac{\int \phi(\nu) J(\nu) d\nu}{\Delta\nu_S \int \frac{\partial \phi}{\partial \nu} J(\nu) d\nu} \right] \equiv T_\alpha, \quad (\text{A13})$$

where we have used that the second term within the square brackets is negligible compared to the first term for all applications in this paper.

A3 The 6-Level Hydrogen Atom with Collisions and CMB photons

In the presence of CMB photons and when collision are accounted for, Eq. (A11) changes to

$$\frac{\partial y}{\partial t} = (1-y) \left(A_{21} + C_{21} + B_{21} I_{\text{CMB}} \right) + (b_1 - b_2) - y \left(4b_1 - b_2 + C_{12} + B_{12} I_{\text{CMB}} \right). \quad (\text{A14})$$

The equilibrium solution in this case is

$$y = \frac{b_1 - b_2 + A_{21} + C_{21} + B_{21} I_{\text{CMB}}}{4b_1 - b_2 + 4C_{21} + 4B_{21} I_{\text{CMB}} + A_{21} - 3C_{21} \frac{T_*}{T_{\text{gas}}}}, \quad (\text{A15})$$

where we used that $B_{12} = 3B_{21}$ and $C_{12} = 3C_{21} e^{-T_*/T_{\text{gas}}} \approx 3C_{21} (1 - T_*/T_{\text{gas}})$, which results in the spin temperature

$$\frac{T_s}{T_*} \approx \frac{3y}{4y-1} = \frac{1 + \frac{C_{21}}{A_{21}} + \frac{B_{21}}{A_{21}} I_{\text{CMB}} + \frac{b_1 - b_2}{A_{21}}}{1 - \frac{b_2}{A_{21}} + \frac{C_{21} T_*}{A_{21} T_{\text{gas}}}} = \frac{1 + \frac{C_{21}}{A_{21}} + \frac{B_{21}}{A_{21}} I_{\text{CMB}} + \frac{b_1(1 + \frac{T_*}{T_\alpha})}{A_{21}}}{1 + \frac{b_1 T_*}{A_{21} T_\alpha} + \frac{C_{21} T_*}{A_{21} T_{\text{gas}}}}. \quad (\text{A16})$$

Since the Ly α scattering rate can be expressed as

$$P_\alpha = 4\pi \int \frac{J(\nu)}{h\nu} \sigma(\nu) d\nu \approx \frac{4\pi}{h\nu_0} \frac{B_{12} h\nu_0}{4\pi} \int J(\nu) \phi(\nu) d\nu = 3A_\alpha \frac{c^2}{2h\nu_0^3} \int J(\nu) \phi(\nu) d\nu \sim \frac{27}{4} b_1, \quad (\text{A17})$$

we recover the standard equation for the hydrogen spin temperature (e.g. Madau et al. 1997):

$$T_s = \frac{T_{\text{cmb}} + y_\alpha T_\alpha + y_c T_{\text{gas}}}{1 + y_\alpha + y_c}, \quad y_\alpha = \frac{4P_\alpha T_*}{27A_{21} T_\alpha}, \quad y_c = \frac{C_{21} T_*}{A_{21} T_{\text{gas}}}. \quad (\text{A18})$$

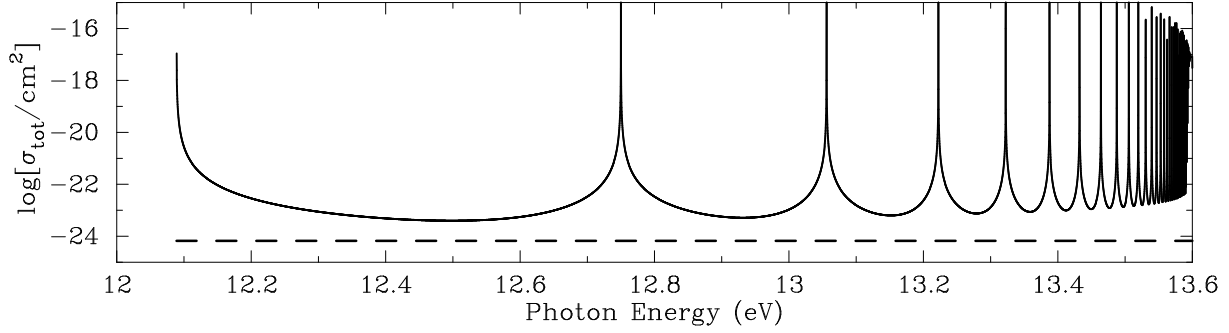


Figure B1. The absorption cross section of neutral atomic hydrogen gas to soft UV photons. The spikes at $E=12.1, 12.8, 13.05, \dots$ correspond to the $\text{Ly}\beta, \text{Ly}\gamma, \text{Ly}\delta, \dots$ -resonances, respectively. The horizontal dashed line corresponds to the Thomson cross-section.

APPENDIX B: THE OPACITY OF GAS TO PHOTONS IN THE ENERGY RANGE $E = 10.2 - 13.6$ EV.

The cross section for $\text{Ly}\alpha$ absorption can be written as

$$\sigma_\alpha(x) = \sigma_{\alpha,0} \phi(x; A_{21}) = f_{12} \frac{\pi e^2}{mc} \frac{1}{\sqrt{\pi} \Delta\nu_\alpha} \phi(x; A_{21}), \quad (\text{B1})$$

where $\sigma_{\alpha,0}$ is the line center cross section, $f_{12} = 0.4167$ the $\text{Ly}\alpha$ oscillator strength and $\phi(x; A_{21})$ is the Voigt function (Rybicki & Lightman 1979, p. 288, Eq. 10.70). The reason for writing the voigt function as $\phi(x; A_{21})$ is that it explicitly demonstrates that it depends on the Einstein A-coefficient (in the wing of the line profile, $\phi(x) = a/[\sqrt{\pi}x^2]$, where $a = A_{21}/4\pi\Delta\nu_D$). Similarly, the cross section for higher order Lyman-series photons can be expressed as:

$$\sigma_n(x_n) = f_{1n} \frac{\pi e^2}{mc} \frac{1}{\sqrt{\pi} \Delta\nu_n} \phi(x_n; A_{n1}). \quad (\text{B2})$$

Here, $x_n = (\nu - \nu_n)/\Delta\nu_n$. To compute the cross sections therefore requires knowledge of the the oscillator strengths, f_{1n} , and the Einstein coefficients, A_{n1} . Menzel & Pekeris (1935) derived the oscillators strengths (Eq. 10.46 in Rybicki & Lightman 1979) to be

$$f_{1n} = \frac{2^9 n^5 (n-1)^{2n-4}}{3(n+1)^{2n+4}}. \quad (\text{B3})$$

From the definition of the oscillator strength we know that

$$\frac{\pi e^2}{mc} f_{1n} = \frac{h\nu_n}{4\pi} B_{1n} = \frac{g_n}{g_1} \frac{h\nu_n}{4\pi} B_{n1} = \frac{g_n}{g_1} \frac{h\nu_n}{4\pi} A_{n1} \frac{c^2}{2h\nu_0^3} \quad (\text{B4})$$

(Rybicki & Lightman 1979, Eq. 10.70). A combination of Eqs. (B3) and (B4) yields A_{1n} .

Given the cross-sections for the various Lyman-series transitions, it is possible to calculate the opacity of neutral gas for a photon of any given energy in the range $E = 10.2 - 13.6$ eV, by summing over all Lyman-series transitions

$$\sigma_\nu = \sum_{i=1}^{\infty} \sigma_i(x_i), \quad x_i = (\nu - \nu_i)/\Delta\nu_i. \quad (\text{B5})$$

The result of this calculation is shown in Figure B1.

APPENDIX C: BLOCKING SOFT UV PHOTONS WITH A HIGH COLUMN OF HYDROGEN

Here we discuss the possibility of filtering out the soft-UV photons, without invoking the presence of dust or H_2 molecules. We consider a bright source which is surrounded by a stationary sphere (or a spherical shell) with a column of neutral hydrogen atoms $N_H \gtrsim 10^{23.5} \text{ cm}^{-2}$. As was shown in Appendix B, at these column densities the sphere is optically thick to all soft UV-photons. The spectrum emerging from such a sphere therefore consists mainly of $\text{Ly}\alpha$ and lower energy photons. In this situation, no $\text{Ly}\alpha$ photons are produced in cascades. Of course, the sphere is also extremely optically thick to $\text{Ly}\alpha$ photons: the line center optical depth to $\text{Ly}\alpha$ photons is $\tau_0 = 2 \times 10^{10} (T_{\text{gas}}/10^4)^{-1/2} (N_H/10^{23.5} \text{ cm}^{-2})$. The $\text{Ly}\alpha$ photons scatter on average $N_{\text{scat}} \sim 2\tau_0$ times before they emerge from the sphere. This introduces a new complication: each time a $\text{Ly}\alpha$ photon excites an atom, there is a finite probability for a collision to put the atom into its $2s$ state. Since atoms in the $2s$ state decay to the ground state ($1s$) via 2-photon emission, this effectively destroys the $\text{Ly}\alpha$ photon. The $2p$ - $2s$ excitation rate through atomic collisions is $C_{2p2s} = 2 \times 10^{-3} n_H \text{ s}^{-1}$ at $T = 10^4$ K (with a negligible temperature dependence, Osterbrock 1962). To reach hydrogen column densities of $N_H \gtrsim 10^{23.5} \text{ cm}^{-2}$ requires the gas density to be high, $n_H \gtrsim 10^2 \text{ cm}^{-3}$. For these densities, $C_{2p2s} \gtrsim 10^{-1} \text{ s}^{-1}$ and the $\text{Ly}\alpha$ escape probability reduces to $P = \exp[-N_{\text{scat}} C_{2p2s}/A_\alpha] \lesssim 0.1$. In reality the escape fraction of $\text{Ly}\alpha$ photons could be even lower. Trace amounts of dust within the obscuring cloud could destroy a large fraction of the $\text{Ly}\alpha$

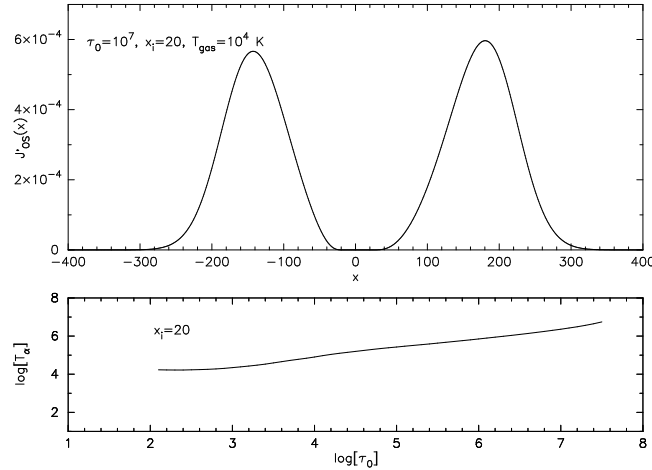


Figure C1. *Top Panel:* The Ly α spectrum 'seen' by a gas element collapsing onto a central Ly α source. The source is also embedded in a static, dense, gas cloud with a hydrogen column density of $\sim 10^{23.5}$ cm $^{-2}$. The spectrum is the blue-shifted 'classical' double peaked spectrum (Eq. C1) suppressed by $e^{-\tau_0\phi(x)}$, with $\tau_0 = 10^7$. The Ly α color temperature associated with this spectrum is $T_\alpha \sim 2 \times 10^6$ K. *Bottom Panel:* The Ly α color temperature as a function of τ_0 . The plot shows that $T_\alpha > 0$ for all values of τ_0 . To couple T_s to T_α , however, requires anomalously large Ly α luminosities.

photons. On the other hand, velocity gradients in the dense cloud would reduce the effective optical depth to Ly α photons, τ_0 , while still blocking the soft-UV photons. This example clearly demonstrates that the escape fraction of Ly α photons is uncertain.

The Ly α photons emerge mostly far in the wings of the line profile. For a static cloud, the emerging Ly α spectrum is symmetric around $x = 0$ and peaks at $x_p = \pm 0.88(a\tau_0)^{1/3} \sim \pm 180(T_{\text{gas}}/10^4)^{-1/3} (\sim \pm 2400(T_{\text{gas}}/10^4)^{1/6}$ km s $^{-1}$, Adams 1972; Neufeld 1990; Dijkstra et al. 2006).⁸ The precise shape of the spectrum depends on where all Ly α are produced. Dijkstra et al. (2006) derived an analytic form of the normalised spectrum ($\int J_{\text{OS}}(x)dx = 1$) in the case all Ly α photons are emitted in the center of a uniform, static sphere

$$J_{\text{OS}}(x) = \frac{2\pi^{3/2}}{\sqrt{24}a\tau_{\text{OS}}} \left(\frac{x^2}{1 + \cosh \left[\sqrt{\frac{2\pi^3}{27}} \frac{|x^3|}{a\tau_{\text{OS}}} \right]} \right), \quad (\text{C1})$$

where τ_{OS} is the total center-to-edge line center optical depth of the sphere (the subscript 'OS' stands for 'obscuring shell/sphere'). In reality, the Ly α photons which are produced in cascades (the 'converted' Ly α photons of § 5.2) are produced more uniformly throughout the sphere, which would slightly enhance the relative number of Ly α photons closer to the line center (Neufeld 1990). However, this does not affect the following discussion. Using the same approach as in § 4, we will demonstrate that the spectrum of Ly α photons in Eq.(C1) cannot give rise to a negative spin temperature in the surrounding gas,. For a gas cloud that is contracting with a constant velocity v_i , the spectrum at the photon front at radius $R_t = ct$ is modified to

$$J'_{\text{OS}}(R_t, t, x) = J_{\text{OS}}(x - x_i)e^{-\tau_0\phi(x)}, \quad (\text{C2})$$

where $x_i = v_i/v_{\text{th}}$ and $\tau_0 = R_t n_N \sigma_0$. In Figure C1, the *top panel* shows $J'_{\text{OS}}(R_t, t, x)$ for $v_i = -20v_{\text{th}} = -260$ km s $^{-1}$, $\tau_0 = 10^7$, and a gas temperature $T = 10^4$ K. The figure shows the spectrum is double-peaked, with an overall blueshift and that photons in the range $x \in [-30, 40]$ are absent. The Ly α color temperature, T_α , associated with this spectrum is $T_\alpha = 2.3 \times 10^6$ K. The reason that the Ly α color temperature, T_α , is positive is that the largest contribution to the denominator of Eq. 7 comes from the photons near $x = -30$ for which $\partial\phi/\partial x > 0$. The *lower panel* shows that the Ly α color temperature is positive for all τ_0 . We can make T_α negative by changing the sign of v_i , which suggests that population inversion may occur in outflows surrounding the thick obscuring slab. However, this requires unphysically large Ly α luminosities. In § 3.2 we showed that in order for $T_s < 0$, $P_\alpha \gtrsim 3 \times 10^{-11}(T_\alpha/[-100 \text{ K}])$ s $^{-1}$. Therefore, for $T_\alpha = -2 \times 10^6$ K (appropriate for $v_i = 20v_{\text{th}}$), the spin temperature is negative only when $P_\alpha \gtrsim 6 \times 10^{-7}$ s $^{-1}$, which according to Eq. (10) requires Ly α luminosities exceeding 10^{48} erg s $^{-1}$ (for reasonable parameters of x_{min} , x_{max} etc). Therefore, blocking soft UV-photons with a large column of neutral hydrogen atoms, does not help in producing maser conditions.

⁸ We point out that the time scale for the Ly α photons to escape from this dense cloud is relatively short, namely $t_{\text{esc}} = (a\tau_0)^{1/3}R/c$, in which R is the radius of the cloud (Spaans & Silk 2006). For a compact dense cloud, the Ly α photons emerge after $t_{\text{esc}} \lesssim 10^6$ yrs. Since this timescale is shorter than the typical lifetime of the quasar phase or star formation episode of galaxies, the associated delay is negligible.